Soft Matter

Accepted Manuscript

ROYAL SOCIETY OF CHEMISTRY

www.rsc.org/softmatter

8/10/2015

Effect of surface charge on boundary slip of various oleophilic/phobic surfaces immersed in liquids

Yifan Li[1,2] and Bharat Bhushan[1,2]*

[1]School of Mechatronics Engineering, Harbin Institute of Technology,

Harbin, 150001, P.R. China

[2]Nanoprobe Laboratory for Bio- & Nanotechnology and Biomimetics (NLBB),

The Ohio State University, 201 W. 19th Avenue, Columbus, OH 43210-1142, USA

Abstract: The reduction of fluid drag is an important issue in many fluid flow applications at the micro/nanoscale. Boundary slip is believed to affect fluid drag. Slip length has been measured on various surfaces with different degrees of hydrophobicity and oleophobicity immersed in various liquids of scientific interest. Surface charge has been found to affect slip length in water and electrolytes. However, there are no studies on the effect of surface charge on slip at solid-oil interfaces. This study focuses on the effect of surface charge on the boundary slip of superoleophilic, oleophilic, oleophobic, and superoleophobic surfaces immersed in deionized (DI) water and hexadecane and ethylene glycol, based on atomic force microscopy (AFM). The surface charge was changed by applying a positive electric field to the solid-liquid interface, and by using liquids with different pH values. Results show that slip length increases with an increase in applied positive electric field voltage. Slip length also increases with a decrease in the pH of the solutions. Change in slip length is dependent on the absolute value of the surface charge, and a larger surface charge density results in a smaller slip length. In addition, the surface charge density at different solid-liquid interfaces is related to the dielectric property of the surface. The underlying mechanisms are analyzed.

Keyword: Boundary slip, Superoleophilic, Oleophobic, Superoleophobic, Hexadecane, Ethylene glycol, Surface charge

*Corresponding author, bhushan.2@osu.edu

1. Introduction

The reduction of fluid drag is of scientific interest in many fluid flow applications, including micro/nanofluidic systems used in biological, chemical, and medical fields.[1] Fluid flow maybe subject to boundary slip at some solid-liquid interfaces, and slip is characterized by the so-called slip length.[2] The boundary slip of surfaces with varying degrees of omniphilicity and omniphobicity have been studied, and slip length in a range of tens of nanometers to several micrometers were reported.[3-9] Published studies also show that the boundary slip condition is believed to affect fluid drag.[10-13]

In aqueous solutions, most solid surfaces could be charged because of either adsorption of ions or dissociation of ionizable groups.[14] The charge at the solid-liquid interface can strongly affect interfacial phenomena. For example, the existence of surface charge at the solid-liquid interface has been found to affect the boundary slip.[9, 15] Further, fluid flow is affected by the interfacial ions distribution[16, 17] and the so-called electrical double layer (EDL) caused by the surface charge at solid-liquid interface based on the electrostatic interaction.[14] This provides a powerful means of drag control. Various modeling and experimental studies have been performed to measure the surface charge density at the interfaces.[9, 18-20]

Applying an external electrical field to the solid-liquid interface and changing the pH of the liquid can both be used to control the surface charge. For surface charges on a solid surface immersed in aqueous solutions with applied electric fields, the surface polarizes in the applied electric field, as free electrons are redistributed to maintain an equipotential. This increases the absolute value of the surface charge with applied negative electric field voltage.[21, 22]

The existence of surface charge is believed to affect the degree of slip. Joly et al.[15] developed a theoretical model regarding the effect of surface charge on slip length based on molecular dynamics simulation. Experimental studies have also been carried out to analyze the effect of surface charge on slip length with applied electric field or liquids with different pH values. Pan and Bhushan[21] studied the effect of electric field on the slip length of a hydrophobic surface immersed in saline solution and deionized (DI) water. They found that the slip length

decreases with the increasing magnitude of the surface charge deposited on the octadecyltrichlorosilane (OTS) surfaces. Jing and Bhushan[9] quantified the surface charge of OTS and a glass surface when immersed in saline solutions with two ionic concentrations, as well as DI water with different pH values. They reported that a larger absolute value of surface charge leads to a smaller slip length.

Liquids with low surface tension, such as oils, are widely used in many fluid flow applications. The study of boundary slip on surfaces immersed in liquids with low surface tension is important with respect to its role on fluid drag. Although boundary slip on superoleophilic, oleophilic, oleophobic, and superoleophobic surfaces immersed in liquids with low surface tension have been studied,[9, 23] the effect of surface charge on the slip length of samples in these liquids has not been reported.

In this paper, the effect of surface charge on the boundary slip of superoleophilic, oleophilic, oleophobic, and superoleophobic surfaces in DI water, hexadecane, and ethylene glycol was studied and analyzed. Because of the wide application of hexadecane and ethylene glycol, these low surface tension liquids were selected. DI water was selected as a reference. The surface charge was changed by applying different external voltage at the solid-liquid interface, and by changing the pH of the liquids. The slip measurements were carried out using an atomic force microscope (AFM) with a colloidal probe.[8, 24, 25] The mechanisms are discussed in this paper.

2. Experimental

The preparation procedures for surfaces and liquids used for the boundary slip study with varying surface charges are introduced first, followed by the measurement techniques. Finally, the methodology for the calculation of slip length is presented.

2.1 Preparation of surfaces

Five samples with different degrees of philicity/phobicity were selected. A hydrophobic and superoleophilic polystyrene (PS) surface is a commonly studied material and was selected. A hydrophobic and oleophilic octadecyltrichlorosilane (OTS) is a self-assembled monolayer with high surface smoothness which minimizes roughness effects and has been studied and was

selected. In addition, three nanoparticle composite coating were selected which were superhydrophobic and superoleophilic, oleophobic, and superoleophobic.

For the preparation of the PS surfaces, a silicon (Si) wafer (Silicon Quest International) with 300 nm thick Si oxide coating grown thermally was used as a substrate. First, the wafer was cleaned by immersion in piranha solution (3:1 mixture of 98% sulfuric acid and 30% hydrogen peroxide) for 30 min. Next, the wafer was rinsed with water and ethanol several times and air dried. A PS solution with concentration of 1% (w/w) was made by dissolving PS pellets (molecular weight 35000, Sigma Aldrich) in toluene (Mallinckrodt Chemical). This was then applied on the Si wafer substrate using the spin coating method at a speed of 2000 rpm. Finally, to remove any remaining solution, the PS coated sample was annealed in an oven at a temperature of 53 ± 2°C for 4 hours.[26]

For the preparation of the OTS surface, a cleaned Si wafer was put into a 1% OTS (v/v) solution (SIO6640.1, Gelest) in anhydrous toluene for 24 hours. Then the wafer was rinsed with toluene several times to remove any unabsorbed molecules from the substrate.[21]

For the preparation of three nanoparticle composite coatings, soda-lime glass (7101, Pearl, China) with 1.0-1.2 mm thickness was used as substrate. For superhydrophobic/superoleophilic surface, SiO_2 nanoparticles and methylphenyl silicone resin binder were used.[27] Tetrahydrofuran (THF) was mixed with isopropyl alcohol (IPA) in a ratio of 40%/60% (v/v). Next, 300 mg of nanoparticles with a diameter of 55±15 nm (AEROSIL RX 50, Evonik Industries) were dispersed into the mixture with a concentration of 10 mg/mL. Then, the nanoparticle suspension was sonicated with a sonifier (Branson Sonifier 450A) at a frequency of 20 kHz and amplitude of 35% for 4 min. After sonication, 150 mg of methylphenyl silicone resin (MPSR) binder (SR355S, Momentive Performance Materials) were added to the nanoparticle suspension and sonicated at the same frequency and amplitude for 4 min. Then, an additional 10 mL of THF/IPA mixture was added to the nanoparticle suspension. After preparation of the nanoparticle solution, dip-coating was used to coat the substrate with a speed of 10 cm/min. Finally, to cure the binder, the surface was annealed in an oven at a temperature of 40 °C for 10 min.

For the preparation of both the superhydrophobic/oleophobic and the superhydrophobic/superoleophobic surfaces, SiO_2 nanoparticle and fluorinated acrylic copolymer binder were used.[28] To prepare superoleophobic surfaces, 300 mg of SiO_2 nanoparticles were dispersed in a 98%/2% (v/v) acetone/formic acid mixture to form a suspension with a concentration of 32 mg/mL. The suspensions were sonicated with a frequency of 20 kHz and amplitude of 35% for 4 min. After sonication, 2200 mg of fluorinated acrylic copolymer (FAC) binder (Dupont) (23% w/w in DI water) was dispersed and sonicated for 4 min. After combination, the nanoparticle to binder ratio was 0.6 by weight and the nanoparticle and binder concentration in the suspension was 8% by weight. Then, a strainer of 0.8 mm pore size stainless steel (070054233, Target Corporation) was used to filter the suspension. After the preparation of the nanoparticle suspension, a spray gun (VL-SET, Paasche Airbrush Company) was used to spray the suspension onto the glass substrate at a distance of about 15 cm and a pressure of 207 kPa. Finally, to cure the binder, the surfaces were annealed in an oven at a temperature of 70 ± 3 °C for 30 min.

To prepare the oleophobic surface, the same materials and processes as for superoleophobic samples were used, except for the ratio of nanoparticle to the binder was reduced from 0.6 to 0.3.

2.2 Liquids

DI water and hexadecane and ethylene glycol, two low surface tension liquids, were selected to study the effect of surface charge on the boundary slip length with an applied electric field voltage. The properties of the liquids used in the experiment are shown in Table 1. DI water and ethylene glycol were selected to prepare solutions with different pH values. Hexadecane was not selected for this experiment because it precipitates when adding trichloroacetic acid (TCA), a liquid used to vary pH.

The pH value of each solution was measured using a pH meter (SG23 SevenGo Duo, Metler-Toledo). The original pH value of ethylene glycol and DI water were measured to be 8 and 7, respectively. DI water was prepared with different pH values in the range of 3 to 11. For

pH < 7, different volumes of 0.01 M TCA water solution were added to the DI water. For pH > 7, different volumes of 0.01 M NaOH water solution were added to DI water.

To prepare the ethylene glycol with different pH values, acid oleic solution and alkaline oleic solution were prepared first. The TCA oleic solution of concentration of 0.1% (v/v) was prepared by dissolving TCA pellets (T6399, SIGMA-ALDRICH) in ethylene glycol (J35756, Mallinckrodt Chemicals), and then sonicating for 10 min to dissolve fully. The NaOH oleic solution with concentration of 0.1% (v/v) was prepared by dissolving NaOH pellets in ethylene glycol, and then sonicating for 15 min to dissolve fully. For pH < 8, different volumes of TCA oleic solution were added to the ethylene glycol. For pH > 8, different volumes of NaOH oleic solution were added to the ethylene glycol. Ethylene glycol with pH values in the range of 3 to 11 was obtained through this process.

2.3 Application of electric field

As shown in **Figure 1**, in order to apply different electric fields, the surfaces were glued to a metal plate using conductive silver paint. The metal plate was also used as an electrode. During the experiment, a stainless steel wire was inserted into the experimental liquid as another electrode. Then, different DC voltages from 0 V to 70 V were applied by a DC power supply (E3612A, HP) to the substrate.

In order to avoid destroying the substrate, the range of voltage for DI water on PS and OTS surfaces was 0 V to 40 V. For DI water on the superhydrophobic/superoleophilic surface, the superhydrophobic/oleophobic surface, and the superhydrophobic/superoleophobic surface, the range was 0 V to 60 V. For hexadecane and ethylene glycol on the all surfaces, the range was 0 V to 70 V. The maximum voltage was dependent on the conductivity of liquids and surfaces.

2.4 Characterization of Surfaces

2.4.1 Morphology of Sample in Air

The morphology of the five surfaces in air was measured using a D3000AFM with a Nanoscope IV controller (Bruker Instruments, Santa Barbara, CA) in tapping mode. A

rectangular N-type Si probe (Forta, Appnano) with a stiffness of 3N/m and a resonance frequency of 66 kHz in air was used. The surfaces were imaged at a scan rate of 0.5 Hz.

2.4.2 CA and CAH measurement

To measure the contact angle (CA) and contact angle hysteresis (CAH) with different surface charges, electric fields and liquids with different pH values were applied to the surfaces. CA and CAH were measured by using a goniometer (290-F4, Ramé-Hart Inc., Succasunna, NJ) and the DROP image software. For CA measurement, a droplet of 5 μL of each liquid was deposited on the surface. Then, an image of the droplet was captured by goniometer and was analyzed by DROP image software. For CAH measurement, a droplet of 5 μL of each liquid was deposited on the sample. Then, the plate was tilted to obtain the advancing and receding CA. The difference between advancing and receding CA was calculated as the CAH.

2.4.3 Electrostatic force and boundary slip measurements using an AFM

An AFM in contact mode was used as shown in **Figure 2**. The colloidal AFM probe was driven towards the surface in liquid at a certain driving velocity and the force detected on the cantilever as a function of the deflection of the cantilever was recorded.

An AFM colloidal probe was used to perform the experiments. To prepare the colloidal probe, a borosilicate sphere (GL018B/45-33, MO-Sci Corporation) with a measured diameter of about 57.6 μm was attached to a rectangular AFM cantilever (ORC8, Bruker) using epoxy (Araldite). Using a large sphere can minimize the hydrodynamic force due to the cantilever because the large sphere increases the separation distance between the cantilever and the surface.[29]

For a flat hydrophilic surface with zero slip, the deflection, *Def*, of the cantilever can be expressed as,[30]

$$Def = \frac{F_{hydro}}{k} = \frac{6\pi\eta R^2}{kD}V \qquad (1)$$

where F_{hydro} is the hydrodynamic force, k is the stiffness of the probe, η is the dynamic viscosity of the liquid, R is radius of the sphere, D is the separation distance between the surface and the bottom of the sphere, and V is the approaching velocity of the sphere. To get F_{hydro} from the

measured value of *Def*, the value of *k* is needed. To measure the stiffness of the probe, the measurement on a hydrophilic Si surface immersed in DI water was carried out. *Def* as a function of the *D* curve was obtained on the Si surface at a long-range distance of 800-1000 nm in which approaching velocity of the probe is expected to remain constant. The data on Si surface to be presented later in **Fig. 5**, was fitted using Eq. 1, and $k/6\pi\eta R^2 = 16.89$ nm s was obtained. Then, for known values of R = 28.8 μm and η = 0.98 mPa s for DI water, the value of *k* was obtained as 0.264 N/m.

For the boundary slip of any hydrophobic surface, the hydrodynamic force can be written in the limit of large separation distance (D >> b) as,[6]

$$\frac{V}{F_{hydro}} = \frac{1}{6\pi\eta R^2}(D + b) \qquad (2)$$

where *b* is slip length. F_{hydro} at a given separation distance *D* is obtained by $F_{hydro} = k \times Def$ using Eq. 1. The slip length can be obtained from the intercept of the curve V/F_{hydro} on the separation distance axis.

For slip length measurement, a driving velocity of 38.5 μm/s was used, and the measured force includes hydrodynamic force and electrostatic force. When the velocity decreases, it leads to a decrease in the hydrodynamic force while the electrostatic force remains constant. When the velocity is low, 0.22 μm/s, the hydrodynamic force on the probe is less than 0.1 nN and can be neglected (can be seen in **Fig. 4** to be presented later). Thus, the measured force can be considered solely as electrostatic force relating to the surface charge, because the hydrodynamic force at low velocity is negligible as compared to the electrostatic force. The increase in surface charge leads to an increase in electrostatic force. Electrostatic force data obtained at low velocity is subtracted from measured force data obtained at high velocity in order to obtain the hydrodynamic force, which is used to obtain slip length.

3 Results and Discussion

High velocity (38.5 μm/s) and low velocity (0.22 μm/s) measurements were made on samples with different applied electric fields and pH values in order to study the effect of electric field and pH values on slip length.

3.1 Morphology and Surface Roughness

Figure 3 shows the 1 μm×1 μm scan size AFM images of all five surfaces in air with root-mean-square (RMS) roughness and peak to valley (P-V) distance calculated. From the images shown in **Fig. 3**, the RMS values and P-V distances of the two hydrophobic surfaces are smaller than that of the three superhydrophobic surfaces. Of the hydrophobic surfaces, the OTS surface has smaller RMS value and P-V distance when compared to the PS surface. Among the three superhydrophobic surfaces, the superhydrophobic/superoleophilic surface has the smallest RMS value and P-V distance, while the superhydrophobic/superoleophobic surface has the largest RMS value and P-V distance. A surface with a high degree of roughness is desirable for superoleophobicity.[31]

3.2 Effect of Electric field

3.2.1 CA and CAH

The CA and CAH of DI water as a function of applied positive voltages from 10 V to 60 V on the five surfaces are shown in Tables 2. For the hydrophobic surfaces deposited with a droplet of DI water, the CA of the droplet on the PS surface decreases from 95 ± 3° to 70 ± 3° with applied voltage from 10 V to 40 V, while the CA of the droplet on OTS surface decreases from 105 ± 4° to 81 ± 2°. The change of CAs with applied electric field can be described by electrowetting using the Young-Lippmann equation,[14, 32]

$$\cos\theta = \cos\theta_0 + \left(\frac{C}{2\gamma_{lv}}\right) E^2 \qquad (3)$$

where θ is the CA of the droplet, θ_0 is the CA in the absence of an electric field, C is the capacitance of the dielectric layer, γ_{lv}, is the liquid-vapor surface tension, and E is the applied voltage.

For the three superhydrophobic surfaces, the CA of the DI water droplet on the surfaces remains constant with the increasing applied voltage from 10 V to 60 V. The reason for the constant CA is the significantly smaller capacitance of these surfaces than that of either PS or OTS. Because the capacitance is inversely proportional to the thickness of the samples, the soda-lime glass substrate with a thickness of 1.0 mm-1.2 mm results in the significantly smaller

capacitance of these surfaces, leading to a significantly smaller change in CA, according to Eq. 3. That change in CA cannot be measured.

The CA and CAH of hexadecane and ethylene glycol as a function of applied voltage did not change as in the case of DI water. Typical data for all samples at 0 V are presented in Table 3.

3.2.2 Electrostatic forces and boundary slip

3.2.2.1 Hydrophobic Surfaces: PS and OTS

(a) Electrostatic forces **Figure 4a** shows the measured electrostatic forces applied on the AFM probe approaching the PS and OTS surface immersed in DI water with different electric fields as a function of separation distance. As in previous studies, the OTS surface in DI water is negatively charged.[33] When a positive electric field is applied to the OTS substrate, the electrostatic force decreases with increasing positive voltage from 0V to 40V. The value of the surface charge decreases with increasing positive voltage. With the applied electric field, there are a certain number of free electrons in the OTS layer between the two electrodes, as shown by Pan and Bhushan.[21] Due to the existence of free electrons, the surfaces polarize in the applied electric field, and free electrons are redistributed to maintain an equipotential. Some of the free electrons move from the top to the bottom of the surface, due to the electrostatic force provided by the electric field. This reduces the negative surface charge density of the interface, and leads to a reduction of the electrostatic force applied on the probe. The electrostatic force of the PS surface is similar to that of the OTS with the increasing applied voltage. However, the amount of change of the electrostatic force for PS is smaller than that of OTS. The reason is that the PS film has a lower capacitance than OTS because the thickness of the PS (about 60 nm) is larger than that of OTS (about 10 nm).[21] Therefore, the change in surface charge on the PS is smaller than that on the OTS surface under the same applied voltage based on $Q = CU$, where Q is the surface charge at the sample, C is the capacitance, and U is the applied voltage.

Figure 4b and **Figure 4c** show the measured electrostatic forces on the AFM probe approaching PS and OTS surface immersed in hexadecane and ethylene glycol with different electric field values as a function of separation distance. For both of the liquids, the change in the

electrostatic force applied on the probe is similar to that of DI water, and the electrostatic forces on the AFM probe decrease with the increasing positive voltage. The results can still be explained by the movement of electrons caused by the applied electric field.

(b) Slip length Slip length is obtained from the hydrophobic forces according to Eq. 2. **Figure 5** shows the effect of applied electric field on the hydrodynamic force, F_{hydro}, applied on the borosilicate glass probe approaching PS and OTS surfaces immersed in DI water, hexadecane, and ethylene glycol at a driving velocity of 38.5 μm/s as a function of separation distance. Measurements on silicon surface was also made as a reference since silicon surface is known to be hydrophilic with zero slip length.

The results of F_{hydro} are similar to the electrostatic force. In order to obtain the slip length, the V/F_{hydro} applied on the AFM probe are presented for PS and OTS surfaces immersed in DI water, hexadecane, and ethylene glycol as a function of separation distance, as shown in **Fig. 6**. In the case of DI water, the plots of V/F_{hydro} on OTS shift to the left with increasing voltage from 0 V to 40 V. This means that the interception of the V/F_{hydro} on the axis of separation distance shifts to the left and leads to the increase of slip length. The plots of V/F_{hydro} on PS in DI water does not have an obvious change. This means that the slip length remains constant. For PS and OTS immersed in hexadecane, the plot of V/F_{hydro} shifts to the left with the increasing voltage from 0 V to 70 V, and leads to a larger slip length. For ethylene glycol, the plots of V/F_{hydro} are similar to that of hexadecane.

Figure 7 shows the slip lengths of PS and OTS surfaces immersed in DI water, hexadecane, and ethylene glycol at zero voltage. Slip length for silicon surface data shown in **Fig. 6** was found to be zero, as expected. **Figure 8** shows the slip length data as a function of applied voltage. With positive electric field applied to the substrate, the slip length of the PS surface in hexadecane and ethylene glycol increases with increasing applied voltage. However, the slip length of PS in DI water remains constant with increasing applied voltage. The slip length of OTS in DI water, hexadecane, and ethylene glycol increases with increasing applied voltage. The

effect of surface charge on the slip length can be given by using the physical model given by Joly et al.,[15]

$$b = \frac{b_0}{1+ (1/\alpha)(\sigma d^2/e)^2(l_B/d^2)b_0} \quad (4)$$

Where b is the slip length considering surface charge, b_0 is the slip length without considering surface charge, α is a numerical factor, σ is the surface charge density, d is the equilibrium distance of Lennard-Jones potential, e is elementary charge, and l_B is the Bjerrum length. The existence of surface charge at the solid-liquid interface will generate an electrostatic force between the solid and liquid, enhance the interaction between the solid and liquid, and reduce the slip length. Here, the decreasing electrostatic force applied on the AFM probe with increasing applied voltage means a decreasing magnitude of surface charge density at the solid-liquid interface. This leads to an increase in the slip length with the increasing applied voltage.

3.2.2.2 Superhydrophobic Surfaces

(a) Electrostatic forces **Figure 9a** shows the measured electrostatic forces applied on the AFM probe approaching the superhydrophobic/superoleophilic and the superhydrophobic/superoleophobic surfaces immersed in DI water with different electric fields as a function of separation distance. Data for the superhydrophobic/oleophobic surface is not shown for brevity. The three superhydrophobic surfaces with SiO_2 nanoparticle coatings are negatively charged in DI water because of the dissociation of the silanol group, as shown in the following equations,[34, 35]

$$SiO_2+2H_2O=Si(OH)_4 \quad (5)$$

$$-SiO_2 \rightleftharpoons -SiO^- + H^+ \quad (6)$$

When a positive electric field is applied to the superhydrophobic/superoleophilic surface, the electrostatic force decreases with increasing positive voltage from 0V to 60V. The absolute value of the surface charge decreases with the increasing positive voltage. Similar results can be found on the superhydrophobic/oleophobic surface and the superhydrophobic/superoleophobic surface. The electrostatic force in the case of the superhydrophobic/oleophobic surface and the superhydrophobic/superoleophobic surface is smaller than that of the

superhydrophobic/superoleophilic surface, and the change in the electrostatic force of all three superhydrophobic surfaces is smaller than that of OTS. The change in electrostatic force of the superhydrophobic/superoleophobic surface is the smallest among the three superhydrophobic surfaces. This is because the concentration of SiO_2 nanoparticle increases from the superhydrophobic/superoleophilic surface to the superhydrophobic/oleophobic surface and the superhydrophobic/superoleophobic surface. The thickness of the coating increases with the increasing concentration of SiO_2 particle, leading to the decreasing capacitance of the surface. This can reduce the effect of applied electric field on the electrostatic force.

Figure 9b and **Figure 9c** show the measured electrostatic forces applied on the AFM probe approaching the superhydrophobic/superoleophilic and superhydrophobic/superoleophobic surfaces immersed in hexadecane and ethylene glycol with different applied voltage as a function of separation distance. For both hexadecane and ethylene glycol, when a positive electric field is applied to the substrate, the electrostatic force has no obvious change with increasing positive voltage from 0 V to 70 V. The absolute value of surface charge remains constant with increasing positive voltage. Thus, it is assumed that when positive electric field is applied, a change of electrostatic force exists, but it is too small to be measured because of the low conductivity of both the liquids and the surfaces. This low conductivity controls the effect of the electric field, so the surface charge does not have an obvious change.

(b) Slip length Slip length is obtained by measuring hydrophobic force. **Figure 10** shows the hydrodynamic force F_{hydro} and V/F_{hydro} applied on a borosilicate glass sphere approaching the superhydrophobic/superoleophilic, and superhydrophobic/superoleophobic surfaces immersed in DI water with different applied voltages obtained at a sphere velocity of 38.5 μm/s as a function of separation distance. For DI water, the plots of V/F_{hydro} for the superhydrophobic/superoleophilic surface shift to the left with increasing voltage from 0 V to 60 V. This means that the interception of the plot on the separation distance shifts to the left and leads to the increase in slip length. A similar result can be found on the other two superhydrophobic surfaces, but the change of V/F_{hydro} for them is smaller than that of the

superhydrophobic/superoleophilic surface. The superhydrophobic/superoleophobic surface has the smallest change in V/F_{hydro} of all the superhydrophobic surfaces.

Figure 7 shows the slip lengths of the superhydrophobic/superoleophilic, superhydrophobic/oleophobic, and superhydrophobic/superoleophobic surfaces immersed in DI water, hexadecane and ethylene glycol at zero voltage. **Figure 11** shows the slip length data as a function of applied voltage values. For the superhydrophobic/superoleophilic surface immersed in the liquids, as shown in **Fig. 11a**, the slip length in the case of DI water increases with applied electric field from 0V to 60V. The slip lengths in the cases of hexadecane and ethylene glycol do not have a change with applied electric field value from 0 V to 70 V. The measured slip lengths of the superhydrophobic/oleophobic surface in DI water, hexadecane, and ethylene glycol are larger than those of the superhydrophobic/superoleophilic surface, as shown in **Fig. 11b**. The changes in slip lengths of superhydrophobic/oleophilic surface and superhydrophobic/superoleophobic surface in DI water, hexadecane, and ethylene glycol with applied electric field are similar to those of the superhydrophobic/superoleophilic surface. It should be noted that, in the case of the superhydrophobic/superoleophobic surface, the error range of the measured value of slip length is larger than that on the other two superhydrophobic surfaces. This can be explained by the higher RMS and P-V distance of the superhydrophobic/superoleophobic surface. The measured slip length is different at the point of the peak than that of the valley on the surfaces, which induces to the larger error range of slip measurement. The change in the slip lengths of the three superhydrophobic surfaces in DI water, hexadecane, and ethylene glycol with the applied voltage can still be explained by the change in the electrostatic force in **Fig. 9** based on Eq. 4.

3.3 Effect of pH value

3.3.1 CA and CAH

Tables 5 and 6 show the CA and CAH of liquids as a function of pH value from 3 to 11 on the all five surfaces. The CAs of DI water and ethylene glycol with different pH value from 3 to

11 do not have an obvious change. This is because the change of CAs with different pH values are too small to be measured.

3.3.2 Slip length

3.3.2.1 Hydrophobic surfaces: PS and OTS

Figure 12a shows the measured slip lengths on PS and OTS surfaces immersed in DI water and ethylene glycol as a function of pH values. For PS immersed in DI water with different pH values, the slip length decreases with the increasing pH value from 3 to 7, and remains constant with the increasing pH value from 7 to 11. For the OTS surface, the slip length decreases with the increasing pH value from 3 to 11. The OTS and PS surfaces immersed in DI water are believed to be negatively charged.[33] When the pH value increases, the increasing concentration of OH^- increases the absolute value of negative charge at the interface. Based on the previous study by Jing and Bhushan,[9] an increase in the surface charge will result in a decrease of the slip length, which is in agreement with this experimental result.

For the PS immersed in ethylene glycol with different pH values, the slip length increases when the pH value increases from 3 to 8, then decreases when the pH value increases from 8 to 11. Similar result can be obtained on the OTS surface. The OTS and PS surfaces immersed in ethylene glycol are also negatively charged by the adsorption of OH^- at the interface. However, the surface charge density is smaller than that in DI water. When the pH value of ethylene glycol changes from 8 to 3, the increasing concentration of H^+ may reduce the negative surface charge to zero at the very beginning. Then, with a further increase of the concentration of H^+, the surface will be subject to an increasing positive charge. This results in the decrease of slip length when the pH value decreases from 8 to 3. When the pH value increases from 8 to 11, the increasing concentration of OH^- promotes the adsorption of OH^- at the interface, increases the absolute value of negative surface charge, and leads to the decrease of slip length.

3.3.2.2 *Superhydrophobic surfaces*

Figure 12b shows the measured slip lengths of the superhydrophobic/superoleophilic, superhydrophobic/oleophobic, and superhydrophobic/superoleophobic surfaces immersed in DI

water and ethylene glycol as a function of pH values. For the superhydrophobic/superoleophilic surface immersed in DI water with different pH values, slip length decreases with the increasing pH value from 3 to 11. Similar results can be obtained on the other two superhydrophobic surfaces. The mechanisms of the change in slip length can still be explained by the effect of pH on the surface charge density at the interface. The three surfaces are also believed to be negatively charged in DI water with the dissociation of the silanol group. The change in pH will affect the dissociation of the silanol group, the surface charge density, and then affect the slip length.

A schematic of the surface charge on the three surfaces immersed in ethylene glycol is shown in **Fig. 13**. When the pH value decreases from 8 to 3, the increasing concentration of OH^- promotes the dissociation of the silanol group and increases the absolute value of the negative charge at the interface. This leads to the decrease of slip length according to Eq. 4. For the superhydrophobic/superoleophilic surface immersed in ethylene glycol with different pH values, slip length increases when the pH value increases from 3 to 8, then decreases when the pH value increases from 8 to 11. It is be believed that when the pH value of ethylene glycol is equal to 8, the negative surface charge density is small, and when the pH value decreases, the surface will be subject to a positive charge. Then, when the pH value changes from 8 to 3 or 8 to 11, the increasing concentration of H^+ or OH^- will increase the absolute value of the positive or negative charge, leading to a decrease of slip length.

4. Conclusions

A colloidal probe AFM was used to study the effect of surface charge on slip length. Experiments with DI water and hexadecane and ethylene glycol, two liquids with low surface tension, on superoleophilic, oleophilic, oleophobic, and superoleophobic surfaces with varying surface charge were carried out. Experiments were carried out on PS (hydrophobic/superoleophilic), OTS (hydrophobic/oleophilic), and three superhydrophobic/superoleophilic, superhydrophobic/oleophobic, and superhydrophobic/superoleophobic surfaces. These were immersed in DI water, hexadecane, and

ethylene glycol with electric voltage value in the range from 0 V to 70 V or pH values in the range of 3 to 11. The underlying mechanisms of the effect of electric field and pH on the surface charge and slip length were discussed. The CAs with the effect of surface charge were measured.

The results of electric field experiments on slip length of the surfaces immersed in liquids showed that the reduction of surface charge affected boundary slip at the solid-liquid interfaces. A smaller absolute value of surface charge leads to larger slip length because movement of free electrons in the surface coatings reduced the electrostatic force. Slip length was not related to CA with increasing applied voltage. Because of the low conductivity of PS in DI water, any change in surface charge was too small to measure. With no observable change in the absolute value of the surface charge, the slip length remained constant. For OTS in DI water, the absolute value of the surface charge decreased with increasing positive electric field values, leading to increased slip length. For these two surfaces in hexadecane and ethylene glycol, the absolute value of the surface charge decreased with increasing positive electric field values, resulting in increased slip length.

The absolute value of surface charge on the three superhydrophobic/superoleophilic, superhydrophobic/oleophobic, and superhydrophobic/superoleophobic surfaces decreased in DI water with increasing positive electric field values, leading to an increase in slip length. In hexadecane and ethylene glycol, the absolute value of the surface charge on these three surfaces remained constant with increasing positive electric field values. The low conductivity of the oils made the charge too small to measure, resulting in a constant slip length.

For the effect of pH on all five surfaces immersed in DI water, the slip length increased when the pH value decreased from 11 to 3 due to the decrease of the negative surface charge. For all five surfaces immersed in ethylene glycol, the slip length increased when the pH value increased from 3 to 8 due to the decrease of positive surface charge. Further, the slip length decreased when the pH value increased from 8 to 11 due to the increase of negative surface charge. Slip length was not related to CA with different pH values.

Acknowledgments

Yifan Li acknowledges financial support from the Chinese Scholarship Council. The authors also like to thank Drs. Yunlu Pan and Dalei Jing for helpful discussions and thoroughly reading the manuscript.

References

1 Bhushan, B. (2010), *Springer Handbook of Nanotechnology, 3rd edition*, Springer-Verlag, Heidelberg, Germany.

2 Navier, C.L.M.H. (1823), "Memoire Sur les Lois du Mouvement Des Fluides," *Memoires de l' Academie Royale des sciences de l' Institut de France* **VI**. 389-440.

3 Tretheway, D. C. and Meinhart, C. D. (2002), "Apparent Fluid Slip at Hydrophobic Microchannel Walls," *Phys. Fluids* **14**, 096105.

4 Bonaccurso, E., Kappl, M., and Butt, H-J. (2002), "Hydrodynamic Force Measurements: Boundary Slip of Water on Hydrophilic Surfaces and Electrokinetic Effects," *Phys. Rev. Lett.* **88**, 076103.

5 Schmatko, T., Hervet, H., and Leger, L. (2005), "Friction and Slip at Simple Fluid-solid Interfaces: The Roles of the Molecular Shape and the Solid-liquid Interaction," *Phys. Rev. Lett.* **94**, 244501.

6 Cottin-Bizonne, C., Steinberger, A., Cross, B. Raccurt, O., and Charlaix, E. (2008), "Nanohydrodynamics: The Intrinsic Flow Boundary Condition on Smooth Surfaces," *Langmuir* **24**, 1165-1172.

7 Bhushan, B., Wang, Y., and Maali, A. (2009), "Boundary Slip Study on Hydrophilic, Hydrophobic, and Superhydrophobic Surfaces with Dynamic Atomic Force Microscopy," *Langmuir* **25**, 8117-8121.

8 Wang, Y. and Bhushan, B. (2010), "Boundary Slip and Nanobubble Study in Micro/nanofluidics Using Atomic Force Microscopy," *Soft Matter* **6**, 29-66.

9 Jing, D. and Bhushan, B. (2015), "The Coupling of Surface Charge and Boundary Slip at the Solid-liquid Interface and Their Combined Effect on Fluid Drag: A Review," *Langmuir* **29**, 6953-6963.

10 Wolynes, P. G. and Deutch, J. M. (1976), "Slip Boundary Conditions and the Hydrodynamic Effect on Diffusion Controlled Reactions," *J. Chem. Phys.* **65**, 450-454.

11 Watanabe, K., Udagawa, Y., and Udagawa, H. (1999), "Drag Reduction of Newtonian Fluid in a Circular Pipe with a Highly Water-repellent Wall," *J. Fluid Mech.* **381**, 225-238.

12 Ou, J., Perot, B., and Rothstein, J. P. (2004), "Laminar Drag Reduction in Microchannels Using Ultrahydrophobic Surfaces," *Phys. Fluids* **16**, 4635-4643.

13 Shirtcliffe, N. J., McHale, G., Newton, M. I., and Zhang, Y. (2009), "Superhydrophobic Copper Tubes with Possible Flow Enhancement and Drag Reduction," *ACS Appl. Mater. Interfaces* **1**, 1316-1323.

14 Israelachvili, J. (1991), *Intermolecular and Surface Forces, 2nd edition*, Academic Press, Inc., London.

15 Joly, L., Ybert, C., Trizac, E., and Bocquet, L. (2006), "Liquid Friction on Charged Surfaces: from Hydrodynamic Slippage to Electrokinetics," *J. Colloid Interf. Sci.* **454**, 152-179.

16 Ajdari, A. and Bocquet, L. (2006), "Giant Amplification of Interfacially Driven Transport by Hydrodynamic Slip: Diffusio-osmosis and Beyond," *Phys. Rev. Lett.* **96**, 186102.

17 Huang, D., Cottin-Bizonne, C., Ybert, C., and Bocquet, L. (2008), "Aqueous Electrolytes Near Hydrophobic Surfaces: Dynamic Effects of Ion Specificity and Hydrodynamic Slip," *Langmuir* **24**, 1442-1450.

18 Bolt, G. H. (1957), "Determination of the Charge Density of Silica Sols," *J. Phys. Chem.* **61**, 1166-1169.

19 Molina, C., Victoria, L., Arenas, A., and Ibáñez, J. A. (1999), "Streaming Potential and Surface Charge Density of Microporous Membranes with Pore Diameter in the Range of Thickness," *J. Membrane Sci*. **163**, 239-255.

20 Hurwitz, G., Guillen, G.R., and Hoek, M.V. (2010), "Probing Polyamide Membrane Surface Charge, Zeta potential, Wettability, and Hydrophilicity with Contact Angle Measurements," J. *Membrane. Sci*. **349**, 349-357.

21 Pan, Y., and Bhushan, B. (2013), "Role of Surface Charge on Boundary Slip in Fluid Flow," J. *Colloid Interf. Sci.* **392**, 117-121.

22 Hughes, C., Yeh, L-H. and Qian, S. (2013), "Field Effect Modulation of Surface Charge Property and Electroosmotic Flow in a Nanochannel: Stern layer effect," *J. Phys. Chem. C*. **117**, 9322-9331.

23 Cho, J-H. J., Law, B. M., and Rieutord, F. (2004), "Dipole-dependent Slip of Newtonian Liquid at Smooth Solid Hydrophobic Surfaces," *Phy. Rev. Lett.* **92**, 166102.

24 Vinogradova, O. I. and Yakubov, G.E. (2003), "Dynamic Effects on Force Measuremnts 2. Lubrication and the Atomic Force Microscope," *Langmuir* **19**, 1227-1234.

25 Zhu, L., Attard, P., and Neto, C. (2011), "Reliable Measurements of Interfacial Slip by Colloid Probe Atomic Force Microscopy. II. Hydrodynamic force measurements," *Langmuir* **27**, 6712-6719.

26 Bhushan, B. and Pan, Y. (2011), "Role of Electric Field on Surface Wetting of Polystyrene Surface," *Langmuir* **27**, 9425-9429.

27 Ebert, D. and Bhushan, B. (2012),"Transparent, Superhydrophobic, and Wear-resistant Coatings on Glass and Polymer Substrates Using SiO_2, ZnO, and ITO Nanoparticles," *Langmuir* **28**, 11391-11399.

28 Muthiah, P., Bhushan, B., Yun, K., and Kondo, H. (2013), "Dual-layered-coated mechanically-durable Superomniphobic Surfaces with Anti-smudge Properties," *J. Colloid Interf. Sci.* **409**, 227-236.

29 Wang, Y., Bhushan B., and Maali, A. (2009), "Atomic Force Microscope Measurement of Boundary Slip on Hydrophilic, Hydrophobic and Superhydrophobic Surfaces," *J. Vac. Sci. Technol. A.* **27**, 754-760.

30 Vinogradova, O. I. (1995), "Drainage of a Thin Liquid-film Confined Between Hydrophobic Surfaces," *Langmuir* **11**, 2213-2220.

31 Bhushan, B. (2012), *Biomimetics: Bioinspired Hierarchical-Structured Surfaces for Green Science and Technology*, Springer-Verlag, Heidelberg, Germany.

32 Quilliet, C. and Berge. B. (2001), "Electrowetting: A Recent Outbreak," *Curr. Opin. Colloid Interface Sci.* **6**, 34-39.

33 Tian, C. S. and Shen, Y. R. (2009), "Structure and Charging of Hydrophobic Material/water Interfaces Studied by Phase-sensitive Sum-frequency Vibrational Spectroscopy," *Proc. Natl. Acad. Sci.* **106**, 15148-15153.

34 Iler, R. K. (1979), *The Chemistry of Silica: Solubility, Polymerization, Colloid and Surface Properties, and Biochemistry of Silica*, Wiley, New York.

35 Behrens, S. H. and Grier, D. G. (2001), "The Charge of Glass and Silica Surfaces," *J. Chem. Phys.* **115**, 6716-6721.

36 Haynes, W. M. (2014), *Handbook of Chemistry and Physics, 95th edition*, Academic Press, New York.

Table 1. Property of liquids used in the experiments[36]

liquid	density (g/cm^3)	surface tension (mN/m)	dynamic viscosity (mPa s)
DI water	0.9970	71.99	0.980
hexadecane	0.7701	27.05	3.032
ethylene glycol	1.1135	47.7	16.100

Table 2. Effect of electric field on the CA, CAH for surfaces immersed in DI water at pH = 7

type of coating	composition	0 V		10 V		30 V		40 V		50 V		60 V	
		CA (deg)	CAH (deg)	CA (deg)	CAH (deg)	CA (deg)	CAH (deg)	CA (deg)	CAH (deg)	CA (deg)	CAH (deg)	CA (deg)	CAH (deg)
Hydrophobic													
superoleophilic	polystyrene (PS)	95±3	27±3	89±3	27±3	75±3	27±3	70±2	28±3				
oleophilic	octadecyltrichlorosilane (OTS)	105±4	39±5	96±1	39±5	85±2	39±5	81±2	38±4				
Superhydrophobic													
superoleophilic	SiO_2 and methylphenyl silicone resin	159±5	7±3	159±5	7±3	158±5	7±3	160±5	7±3	158±5	7±3	158±5	7±3
oleophobic	SiO_2 and fluorinated acrylic copolymer	160±4	12±3	160±4	12±3	160±4	12±3	160±4	12±3	159±4	12±3	155±2	12±3
superoleophobic	SiO_2 and fluorinated acrylic copolymer	162±4	4±1	162±4	4±1	162±4	4±1	162±4	4±1	162±4	4±1	162±4	4±1

pH had no effect on contact angles

Table 3. CA, CAH for surfaces at 0 V immersed in hexadecane (pH = 7) and ethylene glycol (pH = 8)

type of coating	composition	hexadecane		ethylene glycol	
		CA (deg)	CAH (deg)	CA (deg)	CAH (deg)
	Hydrophobic				
superoleophilic	polystyrene (PS)	0		75±3	10±4
oleophilic	octadecyltrichlorosilane (OTS)	33±2	18±3	84±3	15±3
	Superhydrophobic				
superoleophilic	SiO_2 and methylphenyl silicone resin	8±5	2±1	64±2	9±2
oleophobic	SiO_2 and fluorinated acrylic copolymer	100±4	38±6	89±3	22±3
superoleophobic	SiO_2 and fluorinated acrylic copolymer	150±5	11±2	150±7	8±3

pH had no effect on contact angles

igure captions

Figure 1 Schematic of the experimental setup used for measurement of contact angle and slip length as a function of applied voltage.

Figure 2 Schematic of a colloidal AFM probe with sphere approaching relative to a surface and velocity profiles of fluid flow with boundary slip. The definition of slip length *b* characterizes the degree of boundary slip at solid-liquid interface. The arrow above and below the solid-liquid interface represent magnitude and direction for fluid flow.

Figure 3 AFM images in the air, and measured RMS roughness, and P-V distance of (a) two hydrophobic and (b) superhydrophobic/oleophilic, superhydrophobic/oleophobic, and superhydrophobic/superoleophobic surfaces.

Figure 4 Electrostatic force of hydrophobic surfaces immersed in (a) DI water, (b) hexadecane, and (c) ethylene glycol with different applied voltage obtained at a sphere velocity of 0.22 μm/s.

Figure 5 Hydrodynamic force F_{hydro} of a borosilicate sphere on hydrophobic surfaces immersed in (a) DI water, (b) hexadecane, and (c) ethylene glycol with different applied voltage obtained at a sphere velocity of 38.5μm/s.

Figure 6 V/F_{hydro} of sphere on hydrophobic surfaces immersed in (a) DI water, (b) hexadecane, and (c) ethylene glycol with different applied voltage obtained at a sphere velocity of 38.5 μm/s.

Figure 7 A summary of slip lengths for two hydrophobic and three superhydrophobic surfaces immersed in DI water, hexadecane, and ethylene glycol.

Figure 8 Measured slip length on hydrophobic surfaces with different applied voltage to the substrate (A maximum value of 40V was applied in DI water because surfaces were destroyed at a higher voltage, a maximum value of 70V was applied in hexadecane and ethylene glycol because surfaces were destroyed at a higher voltage).

Figure 9 Electrostatic force of superhydrophobic surfaces immersed in (a) DI water, (b) hexadecane, and (c) ethylene glycol with different applied voltage obtained at a sphere velocity of 0.22 μm/s.

Figure 10 F_{hydro} and V/F_{hydro} of sphere on (a) the superhydrophobic/superoleophilicsurface, (b) the superhydrophobic/superoleophobic surface immersed in DI water with different applied voltage obtained at a sphere velocity of 38.5 μm/s.

Figure 11 Measured slip length of superhydrophobic surfaces with different applied voltage to the substrate (A maximum value of 60V was applied in DI water because surfaces were destroyed at a higher voltage, a maximum value of 70V was applied in hexadecane and ethylene glycol because surfaces were destroyed at a higher voltage).

Figure 12 Measured slip length of (a) hydrophobic surfaces and (b) superhydrophobic surfaces immersed in DI water and ethylene glycol with different pH value.

Figure 13 Schematic of the surface charge on the superhydrophobic/surface, the superhydrophobic/oleophobic surface, and the superhydrophobic/superoleophobic surface immersed in ethylene glycol with (a) pH = 8, (b) pH > 8, and (c) pH < 8 value. The left image of figure shows the original status of surfaces in the air when the coating is separate with ethylene glycol. The surface is not charged when (a) pH = 8. When the pH increases to (b) pH > 8, there is an increasing concentration of OH- and lead to an increase of absolute value in surface charge. When the pH decreases to (c) pH < 8, there is an increasing concentration of H^+ that lead to an increase of absolute value in surface charge.

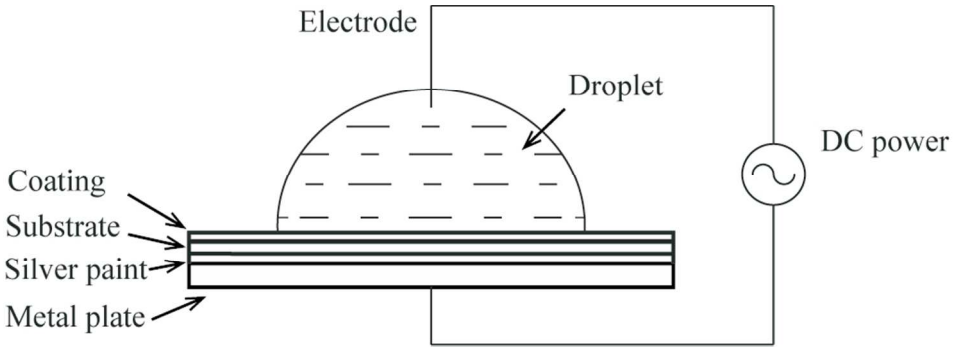

91x31mm (300 x 300 DPI)

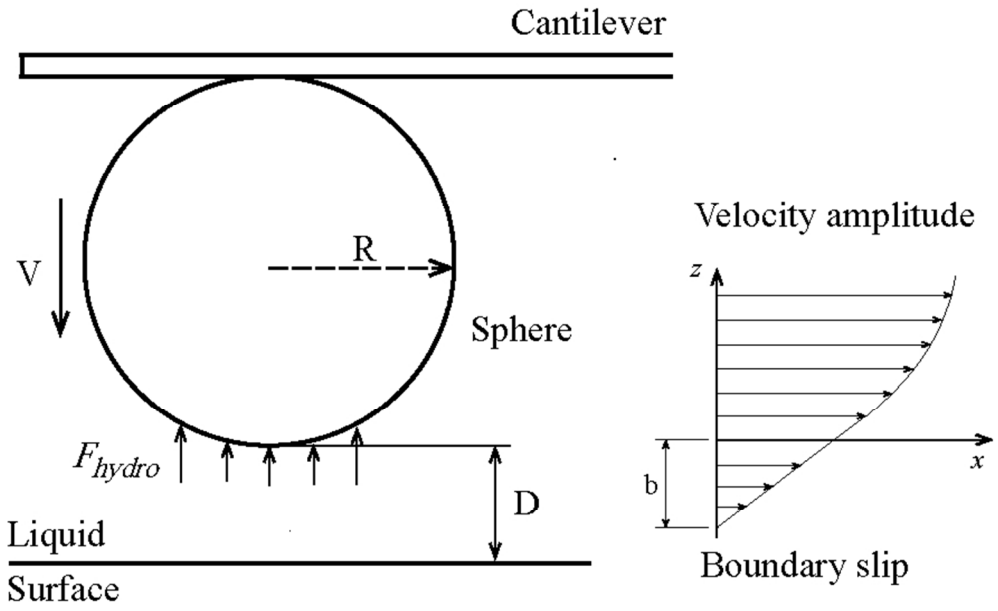

75x46mm (300 x 300 DPI)

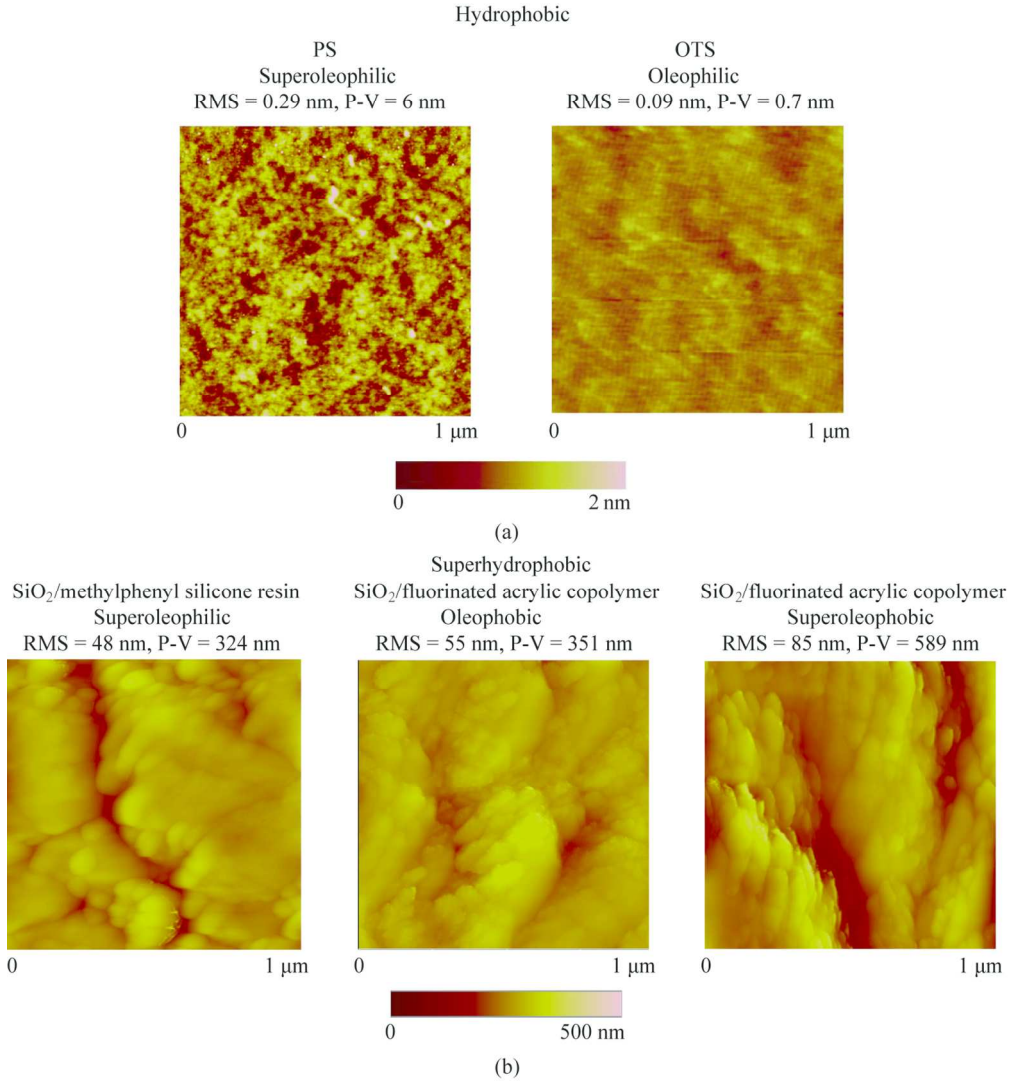

130x140mm (300 x 300 DPI)

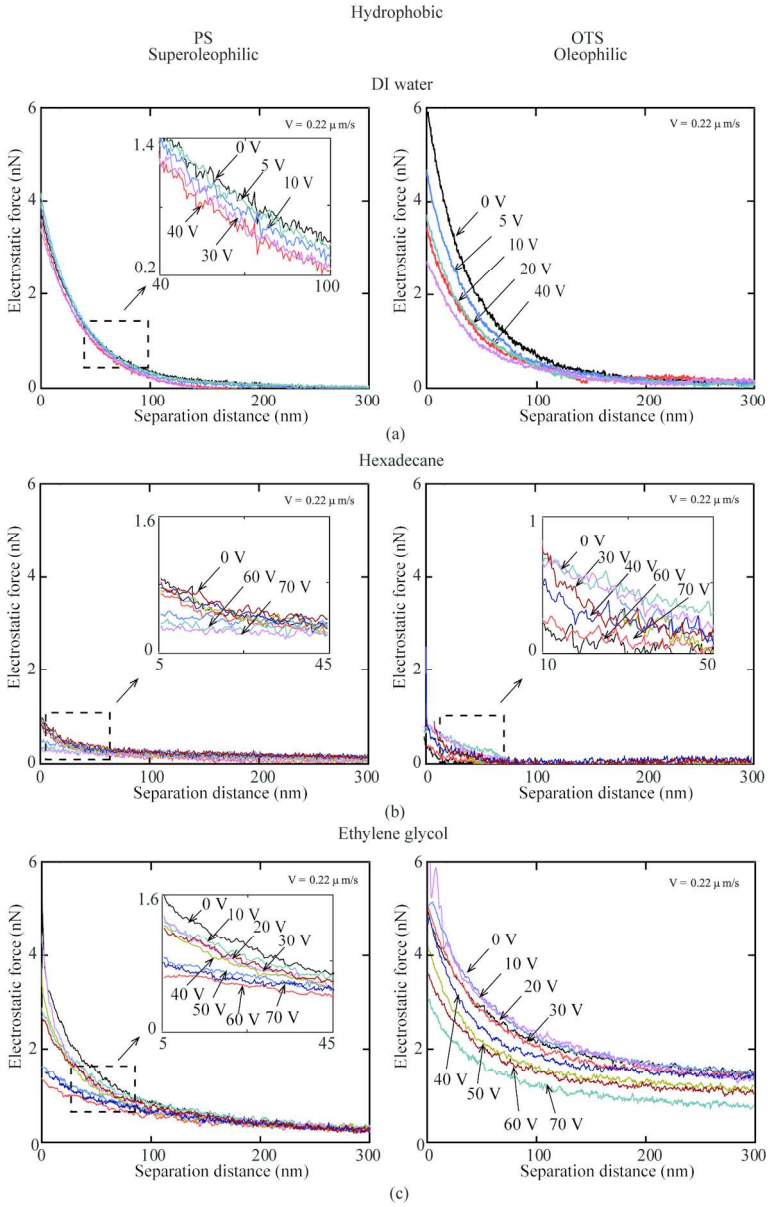

123x194mm (300 x 300 DPI)

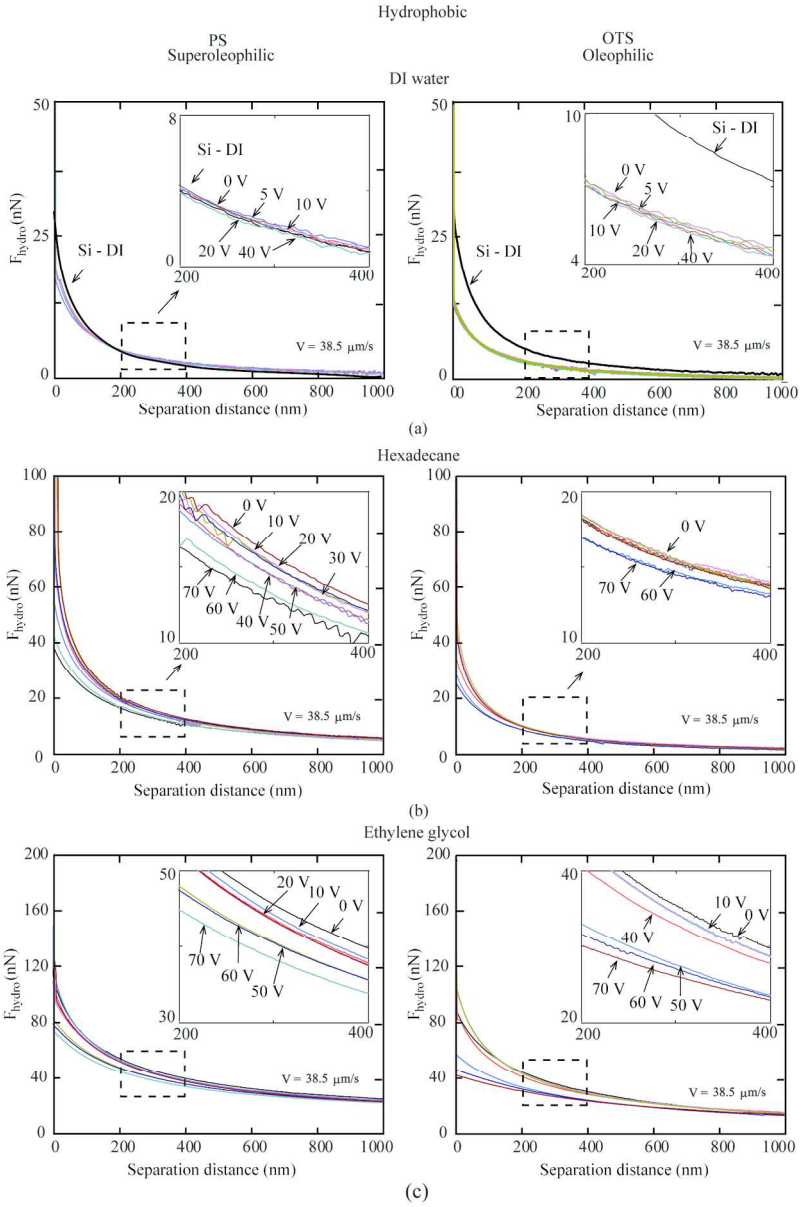

133x200mm (300 x 300 DPI)

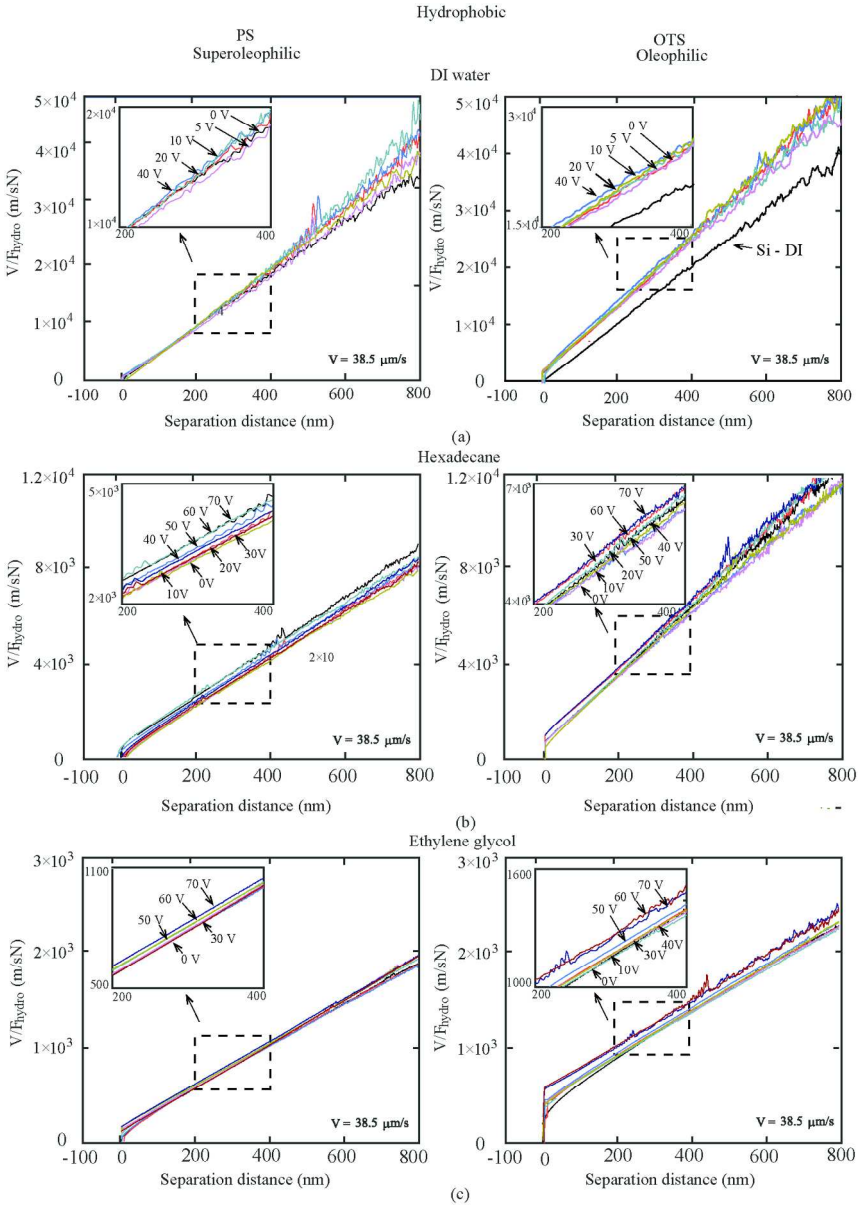

141x199mm (300 x 300 DPI)

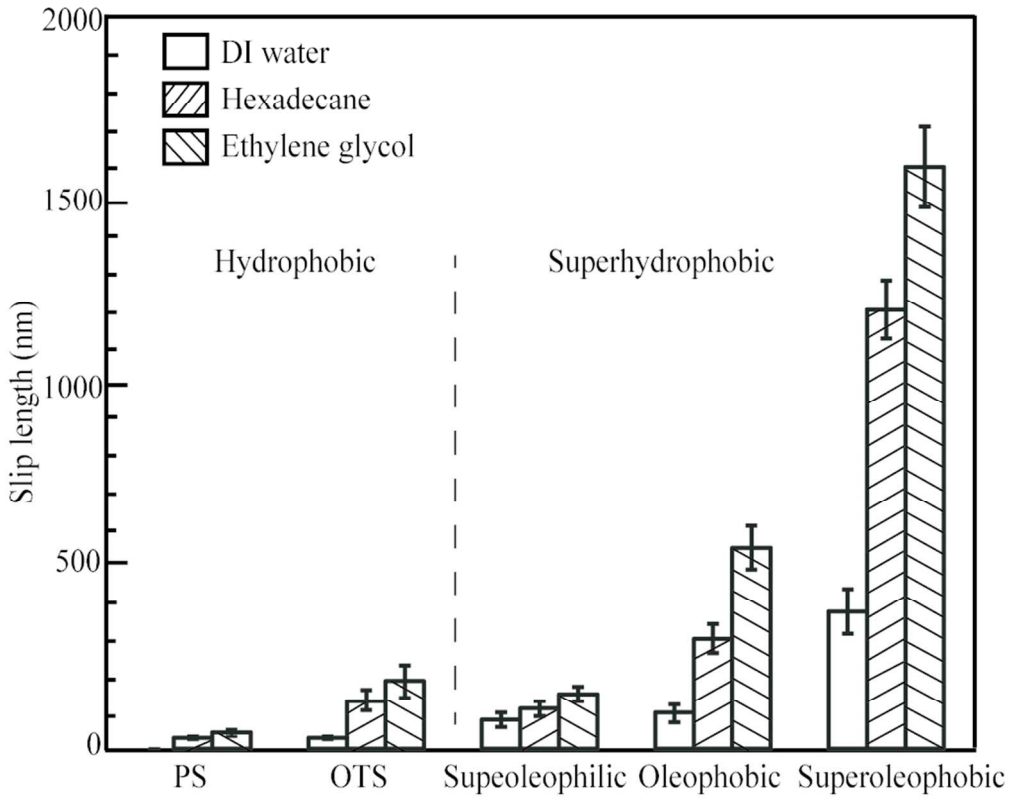

85x68mm (300 x 300 DPI)

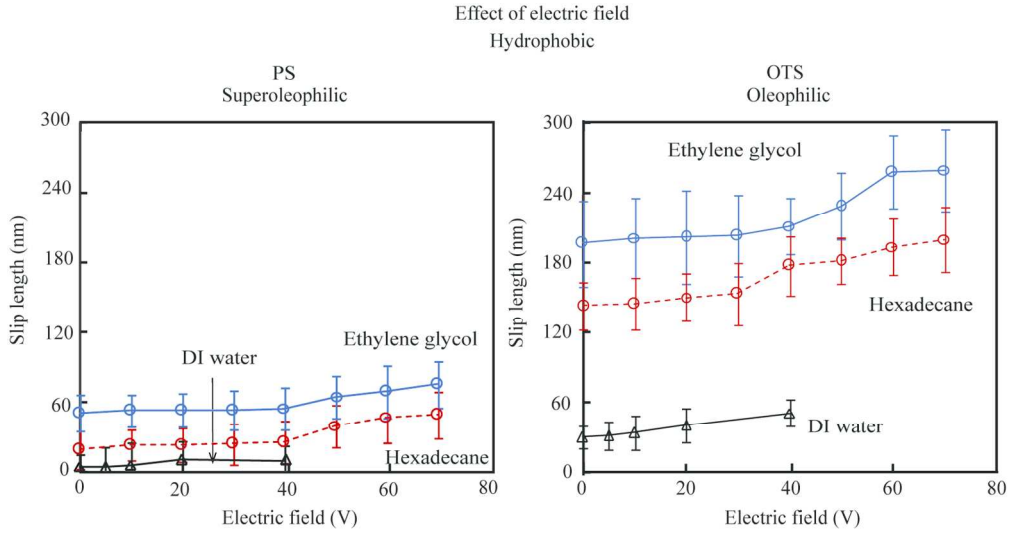

142x74mm (300 x 300 DPI)

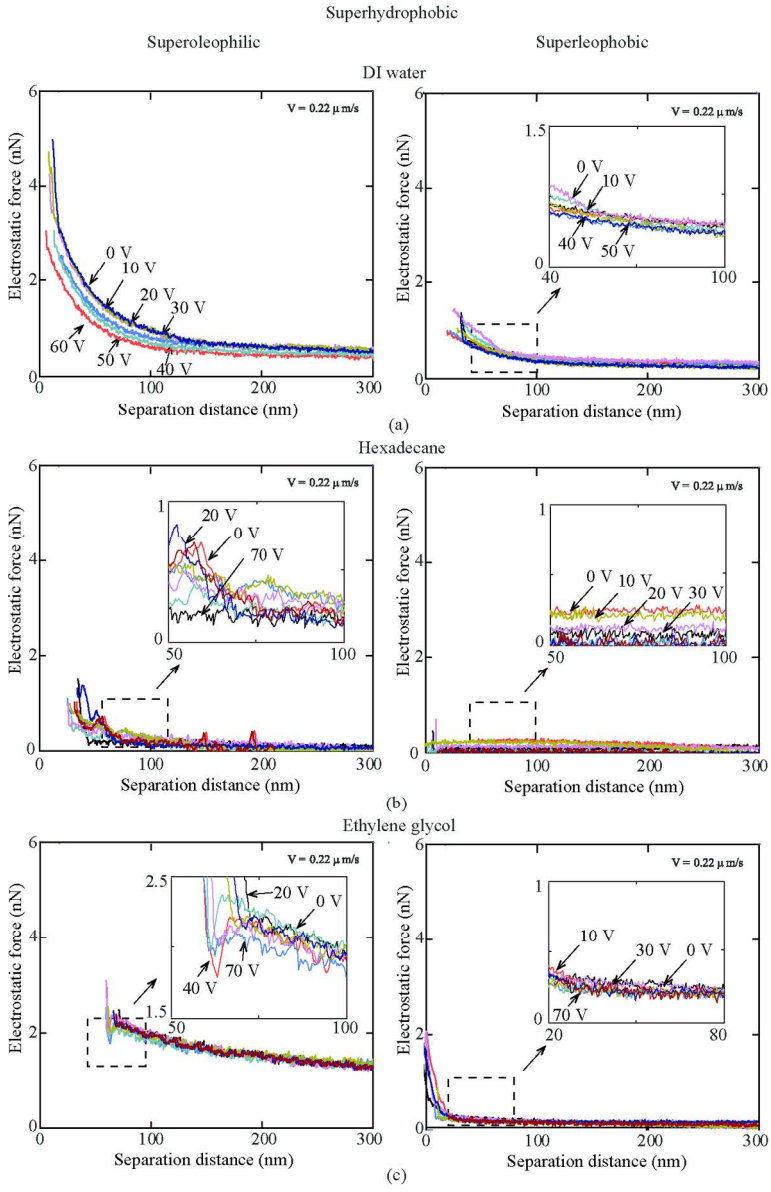

120x188mm (300 x 300 DPI)

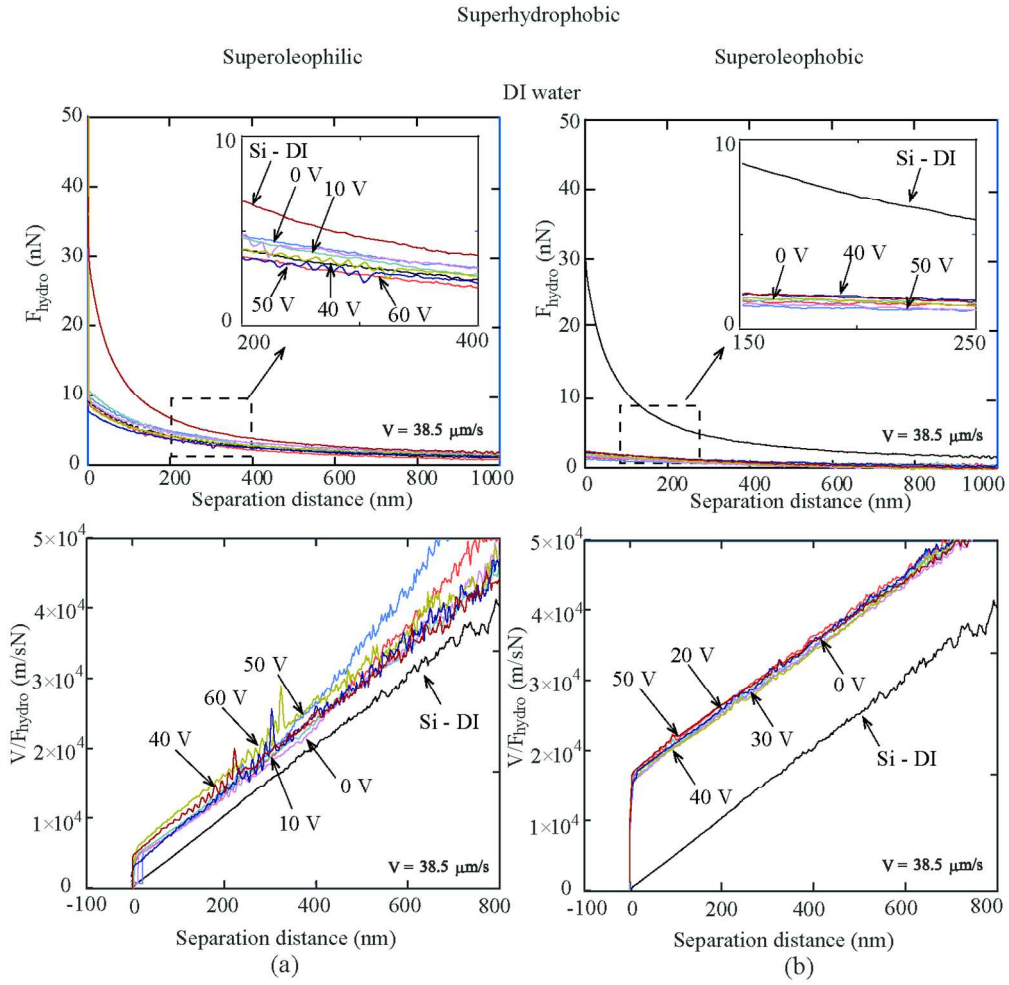

127x125mm (300 x 300 DPI)

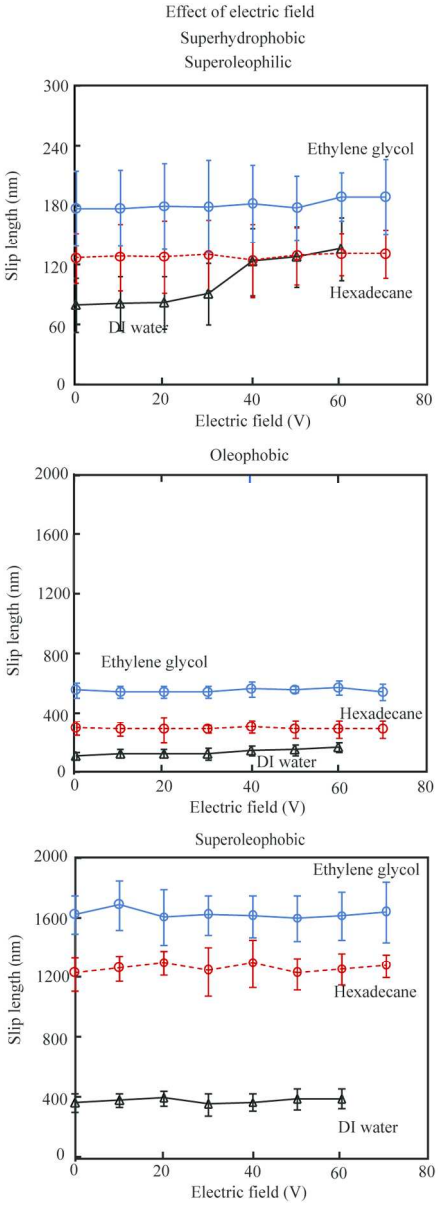

72x199mm (300 x 300 DPI)

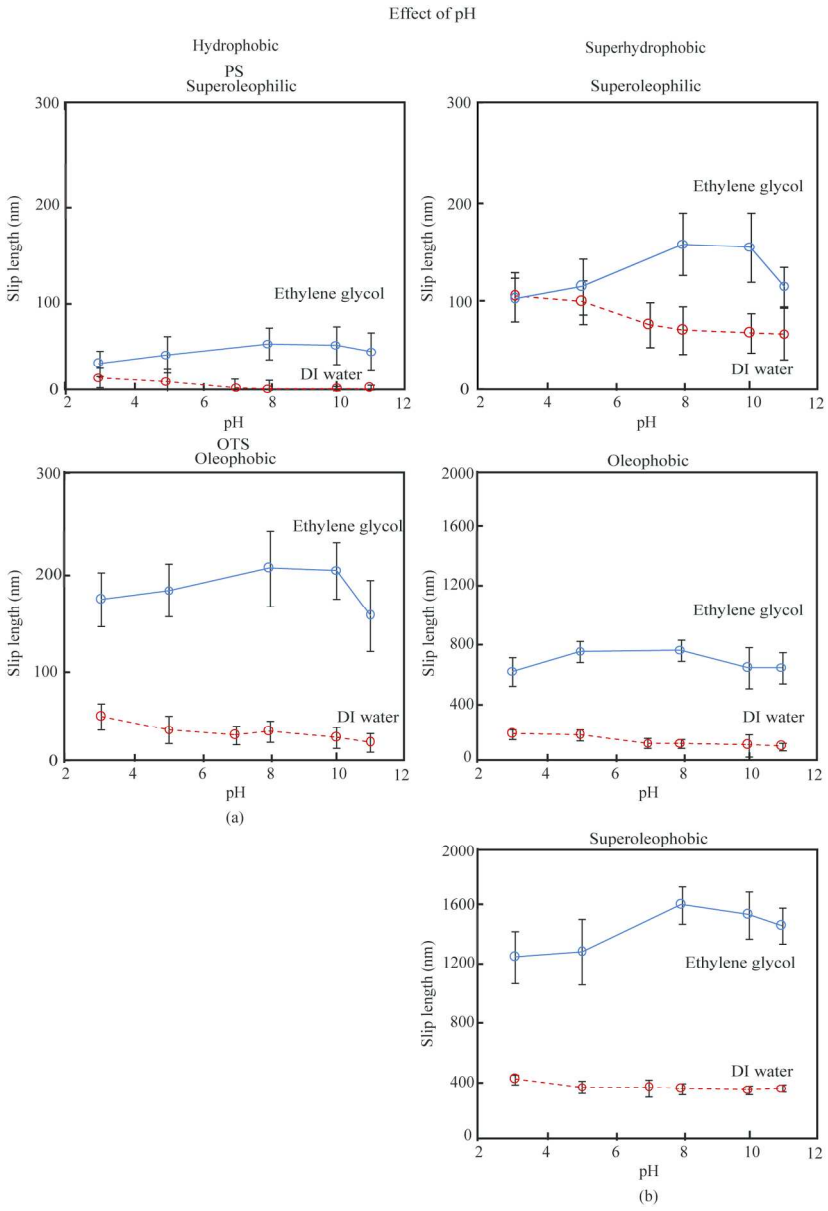

142x207mm (300 x 300 DPI)

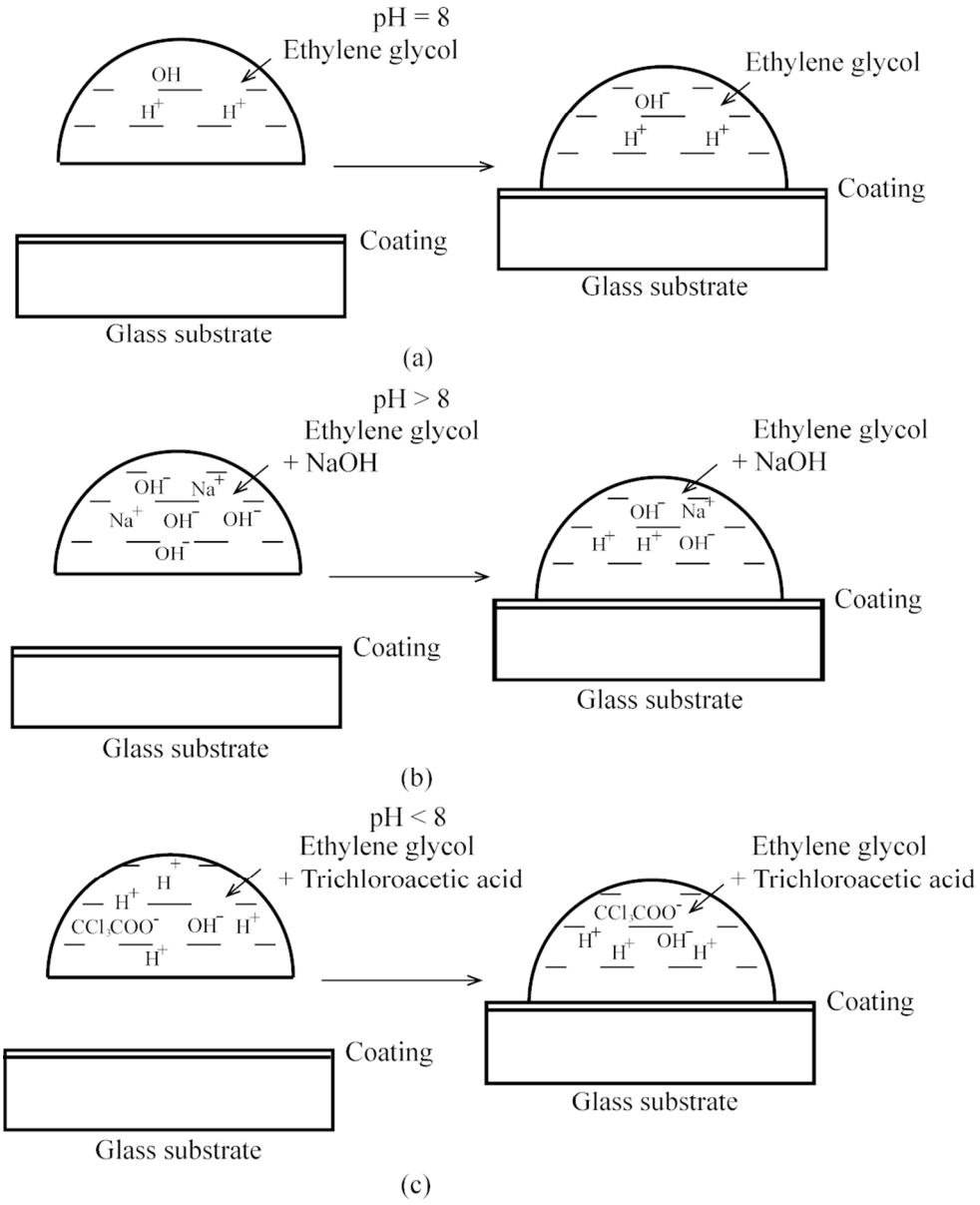

99x122mm (300 x 300 DPI)